

SEVENTH EUROPEAN ROTORCRAFT AND POWERED LIFT AIRCRAFT FORUM

Paper No.7

A Three-Dimensional Approach to Lift and Moment
Coefficients of Rotating Blades

W. Send

DFVLR-Institut für Aeroelastik
Göttingen, Fed. Republic of Germany

September 8 - 11, 1981

Garmisch-Partenkirchen
Federal Republic of Germany

Deutsche Gesellschaft für Luft- und Raumfahrt e.V.
Goethestr.10, D-5000 Köln 51, F.R.G.

A Three-Dimensional Approach to Lift and Moment

Coefficients of Rotating Blades

by

Wolfgang Send

Institut für Aeroelastik der DFVLR
D-3400 Göttingen, Bunsenstr. 10

Summary

The three-dimensional incompressible flow around a thick blade is calculated in the limiting case of an infinitely high Reynolds number. The solution for a four-bladed rotor is achieved by iterating the mutual influence of the induced velocities on the blades. The kinematic motion is forward flight at moderate advance ratio. Several properties of the three-dimensional approach are compared with two-dimensional theories. Unsteady results are obtained by combining the quasi-steady flow with the calculation for a given oscillation mode. The evaluation of the unsteady pressure coefficient leads to the aerodynamic forces.

The integral equation for the flow around the blades is solved by a higher order panel technique for the vorticity vector, which in this particular method is continuous on the blade and downstream in the wake. Though the approach shows some basic features of a three-dimensional rotor, the solution still suffers from an improper description of the wake integral. Required is the induced velocity of a helical sheet of continuously varying vorticity, which is an unsolved problem for the time being. Therefore, the helical wake is substituted by its rectilinear counterpart, which describes at least the near field quite well and for which the author recently found an analytical description.

1. Introduction

It is a well-known fact that the enormous variety of physical phenomena, which accompany the motion of a rotating blade in a compressible fluid, does not allow a consistent description of all occurring effects. A fundamental decision on the way to a mathematical description is required at the point where we adopt the two-dimensional or the three-dimensional point of view. Both of these aspects have their individual advantages with respect to a particular problem in which we might be interested. Basically, the motion of a rotating blade is a three-dimensional process and there seems to be no need to justify a three-dimensional approach. However, the very few residual terms of the initial equations in the final computations deserve some explanatory comments.

The starting point is the theory of unsteady airloads on three-dimensional thick wings in incompressible homogeneous flow. In an earlier paper given at this Forum [1], the details of an higher order panel method applied to the Vorticity Transport Equation (VTE) have already been explained. This method is the computational basis for the calculations presented here. The physical and mathematical simplifications which lead from the underlying VTE to the final equations applied will be discussed later on. The assumptions for the homogeneous flow are maintained and transferred to the rotating blade, except that the kinematics are entirely different. In addition a complete four-bladed rotor is considered. As an example a medium-sized model has been chosen. Its geometric size and data are similar to those of the helicopter BO 105, for which the most complete description could be obtained.

The principal aim is the prediction of the unsteady airloads on the blades and the calculation of the lift and moment coefficients of the rotor in different kinematic conditions. It should be pointed out once again that the solution still suffers from an improper description of the wake integral. Required is the induced velocity of a helical sheet of continuously, harmonically varying vorticity, which remains an unsolved problem.

2. Physical Assumptions

The first two severe restrictions concern the effects of high tip speeds on the advancing blade and reversed flow on the retreating blade. Neither compressibility nor viscous flow are explicitly considered. We adopt the ideas which lead to the so-called potential flow approximation of the conservation laws for mass and momentum in a fluid, which basically is not potential flow, but a simplification of viscous flow for infinitely high Reynolds number.

Fig. 1 summarizes these ideas. As soon as we know the behaviour of the vorticity which is washed down from the blade, we might calculate its induced velocity and solve the integral equation for the boundary condition which requires zero relative velocity inside the moving body.

It is of particular interest to notice that none of the simplifications is really justified for a rotating blade. For the retreating blade the Reynolds number decreases drastically and diffusion is no longer far away. The assumption which leads to Eq. (c) in Figure 1 requires a space-fixed vorticity distribution and is equivalent to a rigid-wake model. A free-wake analysis is the solution of the nonlinear integro-differential equation (b). One must not forget that the velocity \vec{v} in Eq. (b) is the curl of the vector potential, which the vorticity \vec{j} induces and which has to be known simultaneously. For a rotor in vertical flight or forward flight at moderate advance ratio the assumption of a rigid wake is quite appropriate. To obtain an equation which no longer contains the induced velocity field, we neglect the induced velocity in comparison to the kinematic velocity. For a heavily loaded rotor the induced velocity field should not be omitted.

Equation (c) is valid only in nonrotating coordinate systems. With respect to a rotating frame the term $\vec{\omega} \times \vec{j}$ has to be added, where $\vec{\omega}$ is the angular velocity vector. The equation

$$(1) \quad \frac{d}{dt} \vec{j} + \vec{\omega} \times \vec{j} = 0$$

with

$$\frac{d}{dt} = \frac{\partial}{\partial t} + \vec{v}_{rel} \cdot \text{grad}$$

and

$$\vec{v}_{rel} = \vec{v} - \vec{v}_{kin}$$

has to be solved in a blade-fixed coordinate system. All vector components and their arguments are considered to be given with respect to the rotating blade system; \vec{v} is the induced velocity and \vec{v}_{kin} the kinematic motion of the blade. Omitting the induced velocity \vec{v} leads to a semi-linear partial differential equation for the vorticity vector \vec{j} . Semi-linear means linear with respect to the partial derivatives of $\vec{j}(\vec{r}, t)$:

$$(2) \quad \left[\frac{\partial}{\partial t} - \vec{v}_{\text{kin}}(\vec{r}, t) \cdot \text{grad} + \vec{\omega}(t) \times \right] \vec{j}(\vec{r}, t) = 0 \quad .$$

The coefficients in Eq.(2) should contain at least the basic kinematic features, i.e. the translatory motion of the helicopter and the rotation of the blades. Both together form the helical wake. Figure 2 shows the well-known behaviour of \vec{j} in homogeneous flow. The shape of the vorticity distribution in Fig.2c results from a profile with a constant angle of attack. An harmonically oscillating profile produces a time-dependent vorticity, for which the amplitude is shown in Fig.2e.

If we map these two vorticity distributions on a helical wake, the steady case is equivalent to the vorticity produced by collective pitch. A sinusoidal variation of cyclic pitch leads to a cyclic variation of vorticity and is equivalent to Fig.2e. The x-coordinate 2π is reached just after one revolution. Any other kinematic motion or oscillation mode leads to similar wake contributions. Higher harmonics complete one revolution for x equals 4π , 6π , etc. or odd multiples of π .

If we have found a description of the vorticity, the most laborious part of the task has still to be done: calculation of the induced velocity field. The author found recently an analytical description of the three-dimensional wake integral in unsteady homogeneous flow. A brief and preliminary description may be found in Ref.[2]. The integral over a helical wake domain is much more difficult.

The present calculations do *not* contain an helical wake integral; it is substituted by its rectilinear counterpart, which describes at least the near field quite well (Fig.5).

3. Rotor Geometry

The actual geometry of the rotor under consideration is of minor importance, but some information of the modified configuration will be given, which acts as input for the computations (Fig.5). The four blades have a NACA 0012 profile with a constant chord length $x_c = 0.27$ m, and a linearly increasing washout of 8° . For the purposes of aerodynamic calculations there is no need for hinges; the motion of the blades is controlled by the kinematic velocity. The blade root is 1.13 m and the aspect ratio is 14; the pitch axis is at quarter chord. The rotor frequency is 424 rev/min.

4. Kinematics

Though the mathematical description of the kinematics would be able to simulate all possible motions and the program, of course, would deliver an answer, merely vertical flight and forward flight within some reasonable limits are considered.

Figure 3 shows the concepts of the mathematical procedure. The translatory motion of the rotor coordinate system and the rotation of the blades are obtained by successive transformations from a space-fixed system B to a blade-fixed system B*. The details of the transformations are omitted here. The location of a distinguished blade with respect to the plane of rotation is given in Figure 4. In addition to collective and cyclic pitch, which belong to the blade control system, the most important unsteady blade motions are flapping, lagging and feathering motion. Not mentioned in the picture, but also to be added, are the flapwise bending and the torsional motion. It is a fundamental limitation in the approach described here, that the amplitudes of all unsteady motions have to be infinitely small. It is not possible to include any stall effects or to predict other phenomena resulting from finite amplitudes.

5. Mathematical Notes

It has been mentioned already that the mathematical tool for the computations is a higher order panel method developed by the author within recent years. In the present calculations each blade surface consists of 140 panels: 20 panels in circumferential direction and 7 in spanwise direction.

Some calculations have been done with an increased panel size of 30 x 10 panels which shows that the smaller size still gives fairly good results. The pressure coefficient for a thick blade in harmonic motion consists of a purely steady part (index S), an unsteady part (index L) proportional to the amplitude \bar{a} of the particular oscillation mode, and an unsteady part proportional to the square of the amplitude:

$$(3) \quad c_p = \frac{1}{u_0^2} \left(\vec{v}_{kin}^S \cdot \vec{v}_{kin}^S - \vec{v}_{rel}^S \cdot \vec{v}_{rel}^S \right) + \frac{1}{u_0^2} \left(\vec{v}_{kin}^S \cdot \vec{v}_{kin}^L - \vec{v}_{rel}^S \cdot \vec{v}_{rel}^L + \right. \\ \left. + i\omega \phi_D \right) \bar{a} \cdot e^{i\omega t} + \frac{1}{u_0^2} \left(\vec{v}_{kin}^L \cdot \vec{v}_{kin}^L - \vec{v}_{rel}^L \cdot \vec{v}_{rel}^L \right) \bar{a}^2 \cdot e^{i2\omega t}$$

where u_0 is the velocity of the blade tip due to rotation. The kinematic motion is assumed to be built up in a similar manner:

$$(4) \quad \vec{v}_{\text{kin}}(\vec{r}, t) = \vec{v}_{\text{kin}}^S + \vec{v}_{\text{kin}}^L(\vec{r}) \frac{1}{a} e^{i\omega t} .$$

\vec{v}_{rel}^S and \vec{v}_{rel}^L are solutions of the integral equation for the flow problem, which also delivers the doublet potential ϕ_D .

One particular problem should be mentioned, although a discussion is beyond the scope of this paper. Any rotational motion does not fulfill the basic assumption of irrotational flow, which presupposes the existence of the scalar potential ϕ_D . This statement holds also for the simple pitching motion in homogeneous flow. Vanishing relative velocity inside a body necessarily leads to the equation $\vec{v} = -\vec{v}_{\text{kin}} = -\text{grad } \phi_D$, which is undoubtedly wrong for any rotational motion.

6. Results

To demonstrate the present capability of the program, as one example for the aerodynamic forces, the spanwise lift distribution has been selected. Two flight conditions are considered: vertical flight (ascending at 4 m/s) and forward flight (horizontal velocity 60 m/s ; advance ratio $\mu = 0.27$). The blade position is $\psi = 90^\circ$ for all cases considered (c.f. Figure 4).

All lift coefficients are given with respect to unit chord length and per meter in spanwise direction. The exerted thrust $T(y)$ is given by

$$(5) \quad T(y) = q_0 \cdot x_c \cdot c_a(y)$$

with

$$q_0 = \frac{1}{2} \rho_0 u_0^2 ,$$

$$\rho_0 = 1.2 \text{ kg m}^{-3} ,$$

$$u_0 = 218 \text{ ms}^{-1}$$

and represents the blade force normal to the plane of rotation.

In Figure 6 the solid line belongs to a collective pitch angle of $\theta_0 = 11.6^\circ$. At this angle the rotor thrust just balances the total weight of the helicopter.

The assumed mass is 2300 kg . The dashed line differs from the solid line by an increased number of panels. If the washout of 8° is suppressed, a collective pitch angle of $\theta_0 = 6.4^\circ$ produces the same mean lift as in the previous case. For comparison the lift distribution in homogeneous flow is shown, which again has the same mean lift (angle of attack: 2°). The forward flight case is an untrimmed flight condition. The collective pitch angle is $\theta_0 = 11.2^\circ$ and the cyclic pitch angle $\theta_0 = 4.2^\circ$.

It turned out during the computations that, except for vertical flight, a trimmed flight condition requires extensive calculations and should be gained by means of a trim program, which gives some approximated values for the final calculations.

Figure 7 shows the relative velocity field on the blade for the vertical flight case in chordwise direction. The values are normalized by u_0 . The domain for negative $x \in [-1,0]$ covers the lower side of the profile from the trailing edge to the leading edge. The peak at the tip ($x = 0$, $y/R = 1.0$) might be responsible for the formation of the tip vortex.

For the unsteady airloads two cases are considered in Figures 8 and 9: feathering and flapping motion. The natural reduced frequency ω_0^* of the unsteady motion is given by

$$(6) \quad \omega_0^* = \frac{\Omega \cdot x_c}{2 u_0} = 0.053 \quad .$$

The chosen value of $\omega^* = 0.1$ is close to the first harmonic. The unsteady thrust $\bar{T}(y,t)$ is given by

$$(7) \quad \bar{T}(y,t) = [\text{Re}(c_a(y)) + \text{Im}(c_a(y))] \cdot \bar{a} \cdot x_c \cdot e^{i\omega t}$$

where \bar{a} is the amplitude of the unsteady motion and ω the circular frequency. For the flapping motion the amplitude is assumed to increase from zero at the blade root to \bar{a} at the blade tip. The corresponding values for homogeneous flow are based on a steady flow field resulting from 2° angle of attack (c.f. Figure 6).

7. Conclusion

The first components of a program to compute unsteady airloads in rotating systems have been developed within the last two years at the DFVLR-Institute of Aeroelasticity. Though the capability is still confined to incompressible flow, the calculation of unsteady lift and moment coefficients is now possible within the limits outlined in the present paper. Nevertheless the constraints are still quite numerous and a wide range of application requires first of all an unsteady wake integral with a helical geometry, which is an enormous project with many inherent uncertainties.

The theory of higher order panels for the vorticity vector has proved to give very reliable results. However, an extension to a more flexible geometry is desired. Presently a precise calculation of different tip shapes is hardly possible.

Finally, it should be pointed out that the calculation of compressibility effects is less difficult than might be expected. As soon as the total derivative of the pressure with respect to time is known in the surrounding flow field for the incompressible fluid, a first order computation of Mach number effects is possible. Some preliminary considerations in this direction have been made within the last year.

8. References

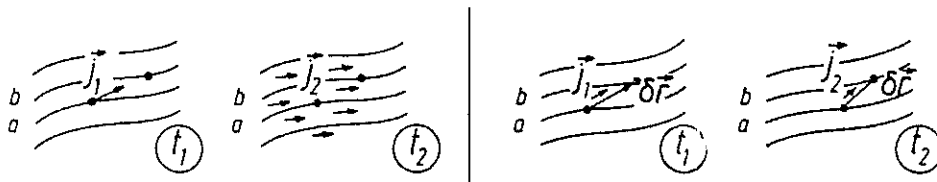
1. Send, W. Higher Order Panel Method Applied to Vorticity Transport Equation.
Fifth European Rotorcraft and Powered Lift Aircraft Forum, Amsterdam, 1979.
2. Send, W. Analytical Representation of the Three-Dimensional Wake Integral in Unsteady Flow.
Proceedings of the Colloquium honoring Hans Georg Küssner on the occasion of his 80th birthday, Göttingen, Sept.24, 1980.

$$\frac{d}{dt} \vec{j} = \vec{j} \cdot \text{grad } \vec{v} + \nu \Delta \vec{j} \quad (a) \quad + \quad \text{Boundary condition } \vec{v}_{\text{rel}} = 0$$

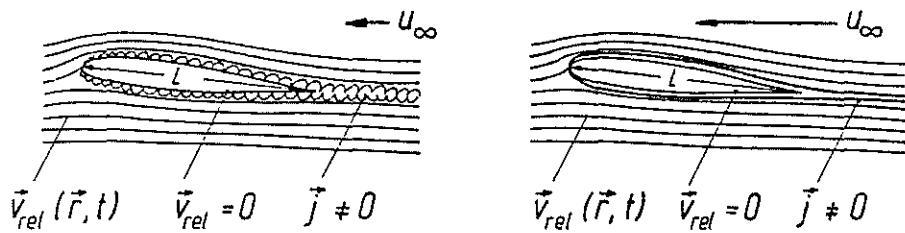
Change of \vec{j} with respect
to time to space

Transportation Diffusion

Relative position
vector $\delta \vec{r}$ $\frac{d}{dt} \delta \vec{r} = \delta \vec{r} \cdot \text{grad } \vec{v}$
Differential Eq.



low \updownarrow Reynolds Number $Re = \frac{U_\infty \cdot L}{\nu}$ \updownarrow high



(a) \rightarrow $\frac{d}{dt} \vec{j} = \vec{j} \cdot \text{grad } \vec{v}$ (b) \rightarrow $\frac{d}{dt} \vec{j} = 0$ (c) \rightarrow
(diffusion far away) (no change of \vec{j} with respect to space)

$\vec{v}_{\text{rel}} \approx \begin{bmatrix} U_\infty \\ 0 \\ 0 \end{bmatrix} \rightarrow \left(\frac{\partial}{\partial t} + U_\infty \frac{\partial}{\partial x} \right) \vec{j} = 0$ (d) $\Rightarrow \vec{j}(\vec{r}, t) = \vec{j}(U_\infty t - x, y, z)$ (e)
Solution

Figure 1: Vorticity Transport Equation
Physical Simplifications

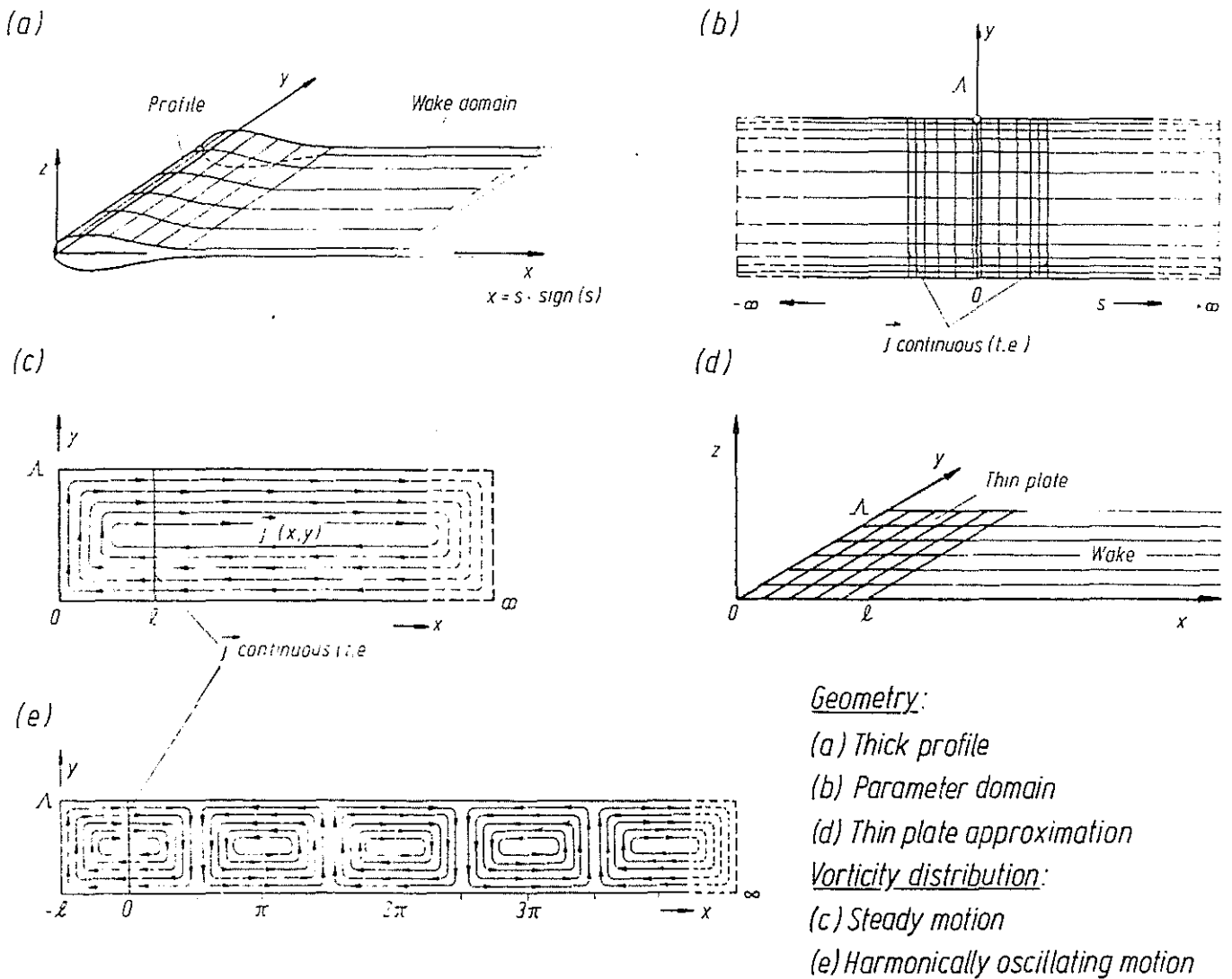


Figure 2: Rigid Wake Model in Homogeneous Flow

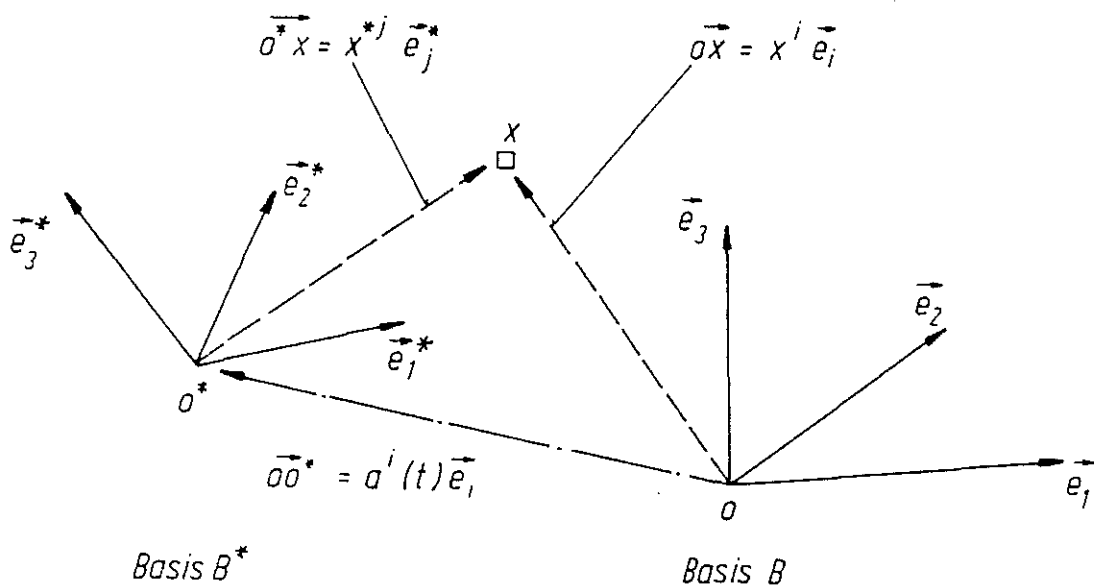


Figure 3: Accelerated and Space-Fixed Coordinate System

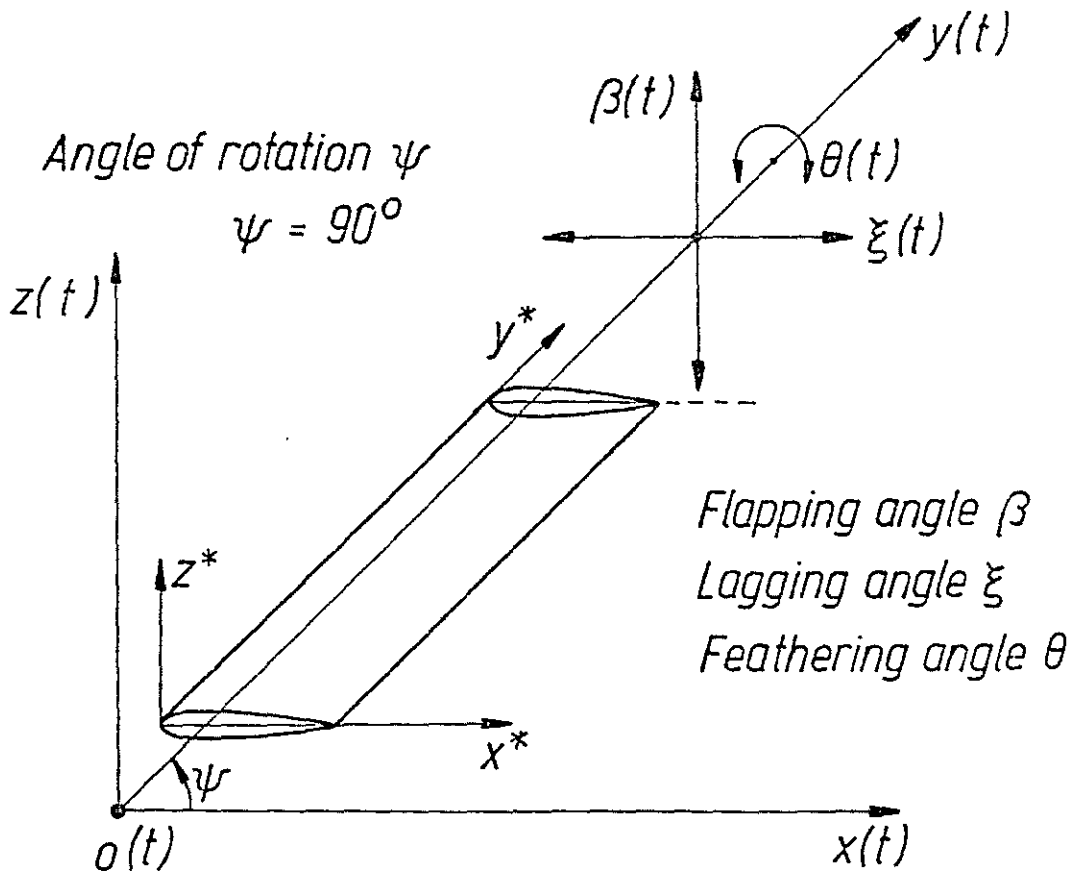
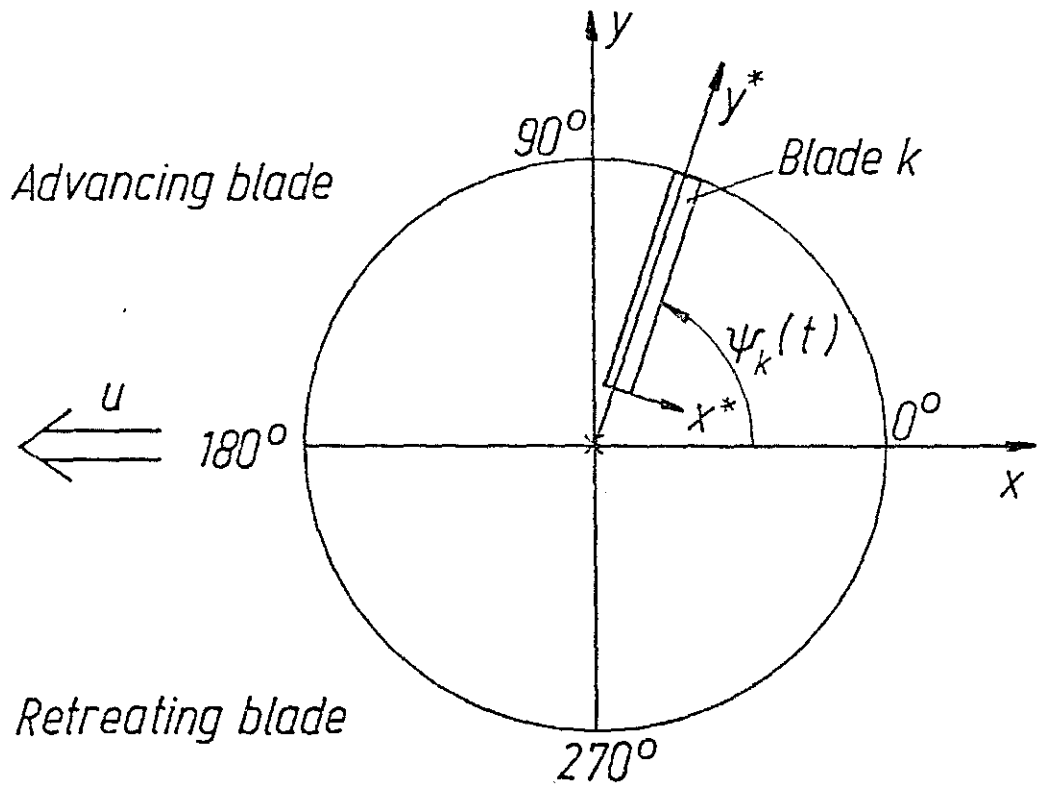


Figure 4: Blade-Fixed Coordinate System (Basis B^*)

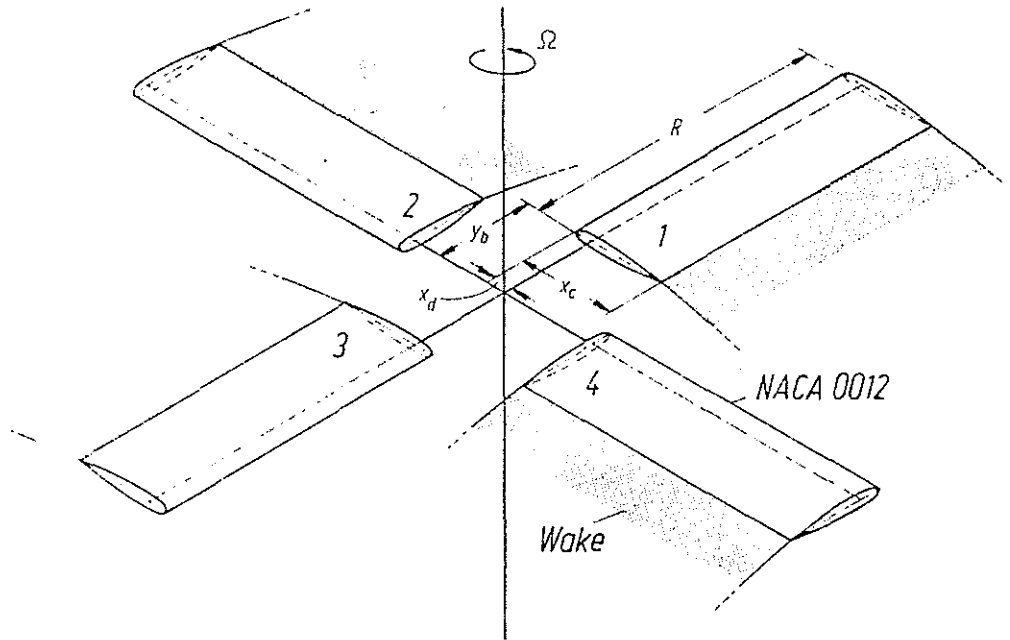


Figure 5:
Wake Model for
a Four-Bladed Rotor

$$\begin{aligned}\Omega &= 44.4 \text{ s}^{-1} \\ x_c &= 0.27 \text{ m} \\ R/x_c &= 14\end{aligned}$$

$$\begin{aligned}y_b &= 1.13 \text{ m} \\ \text{twist} &= -8^\circ \text{ linear} \\ x_d/x_c &= 0.25\end{aligned}$$

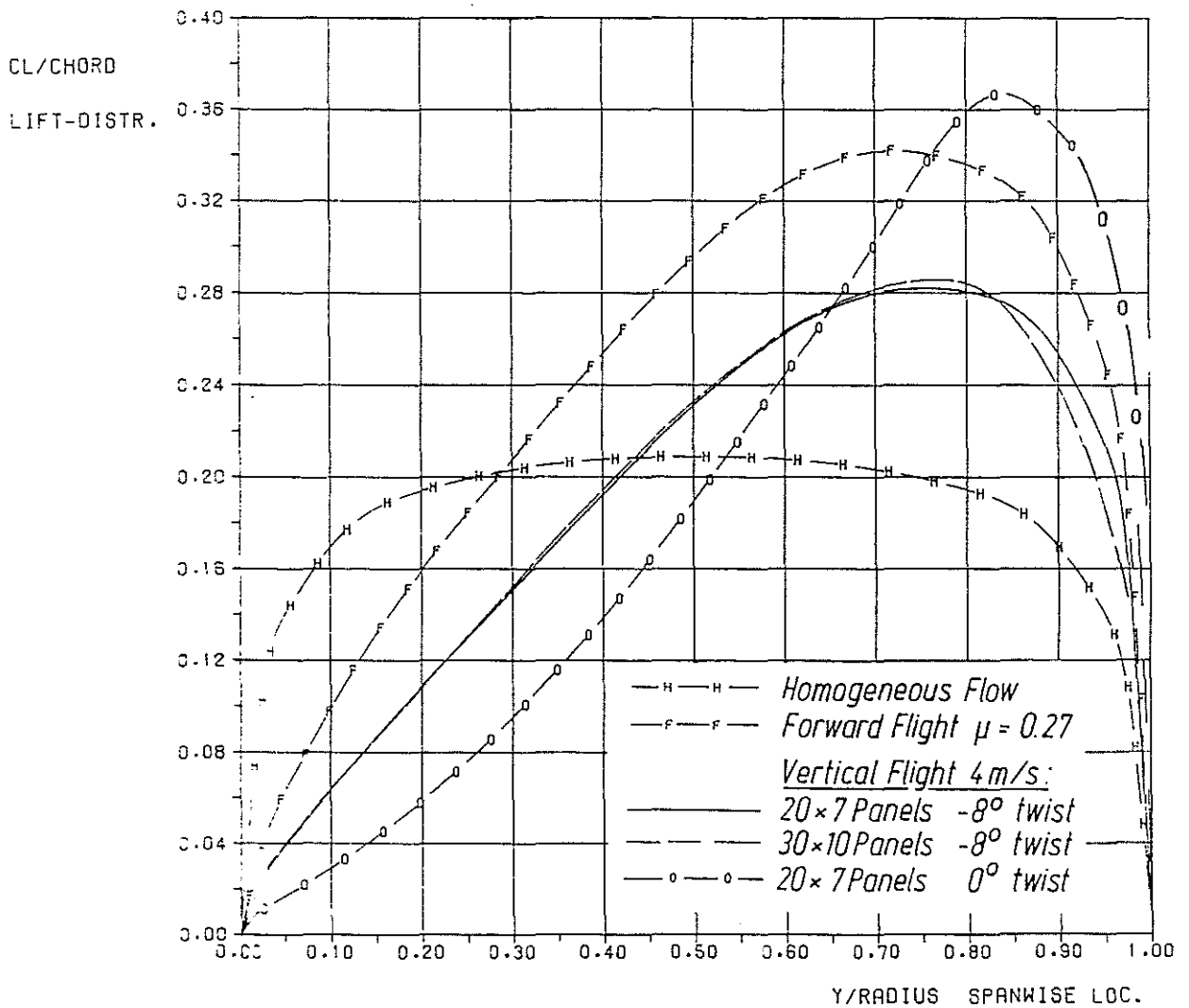


Figure 6: Spanwise Lift Distribution

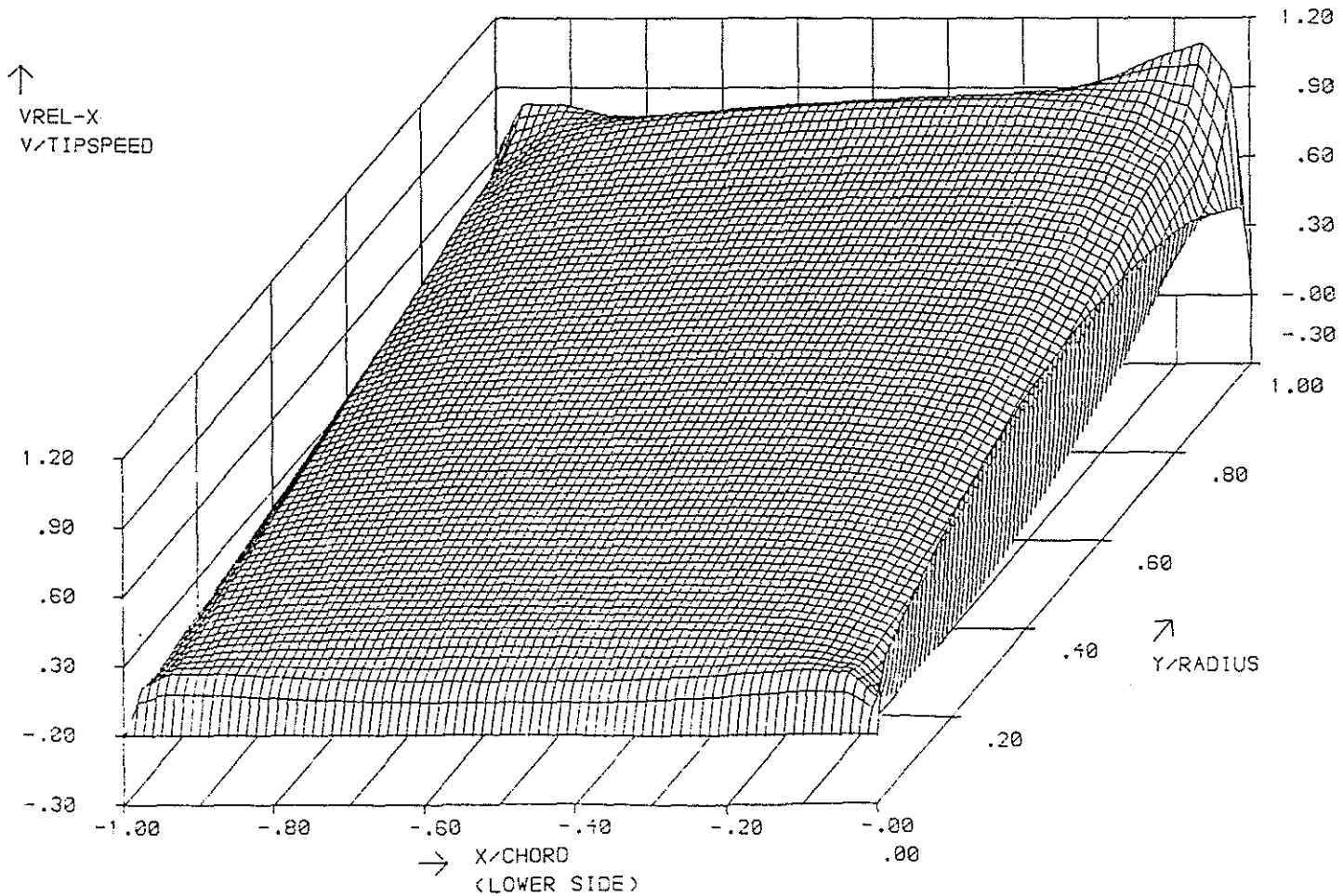
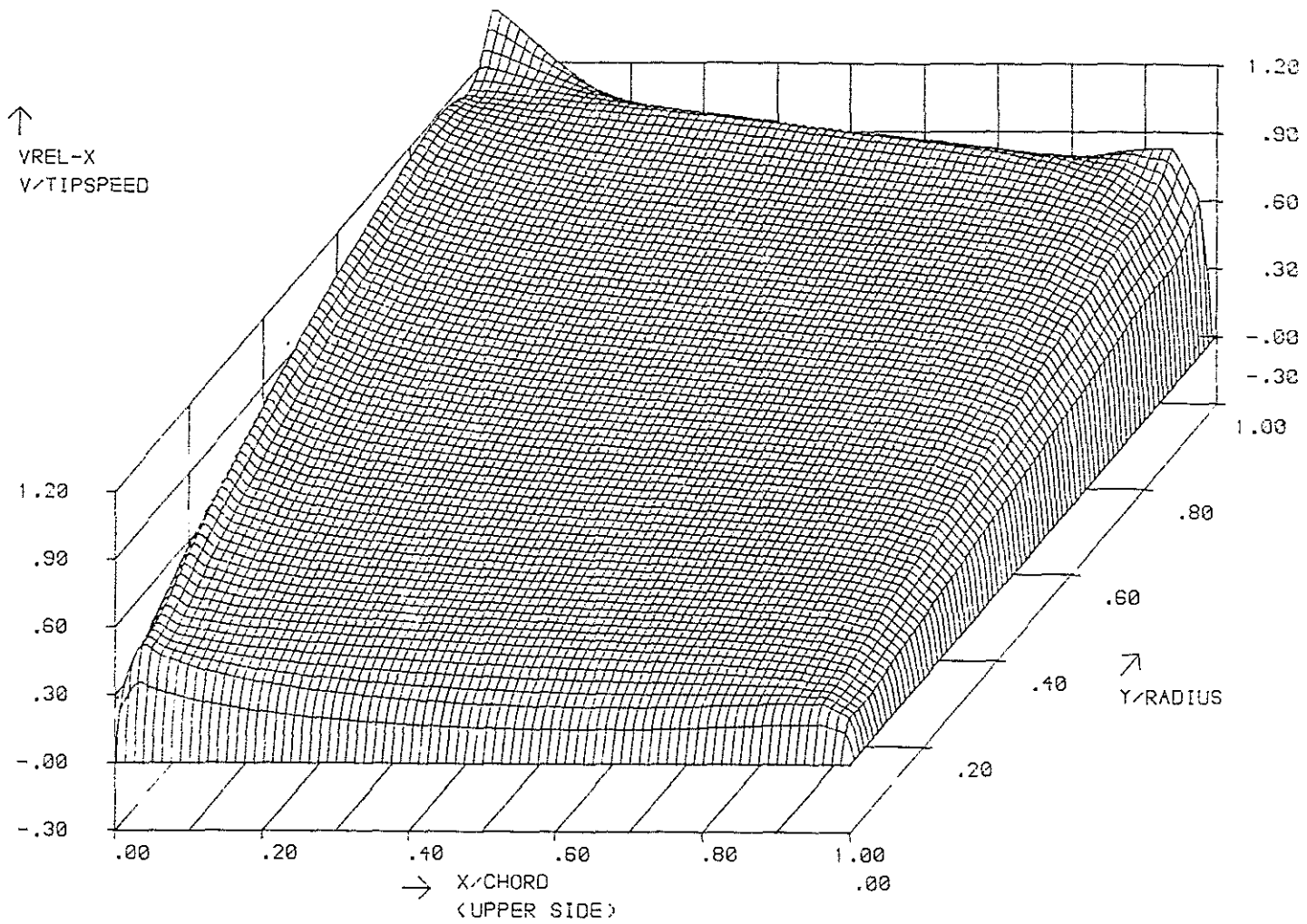


Figure 7: Relative Velocity \vec{v}_{rel} (Advancing Blade)

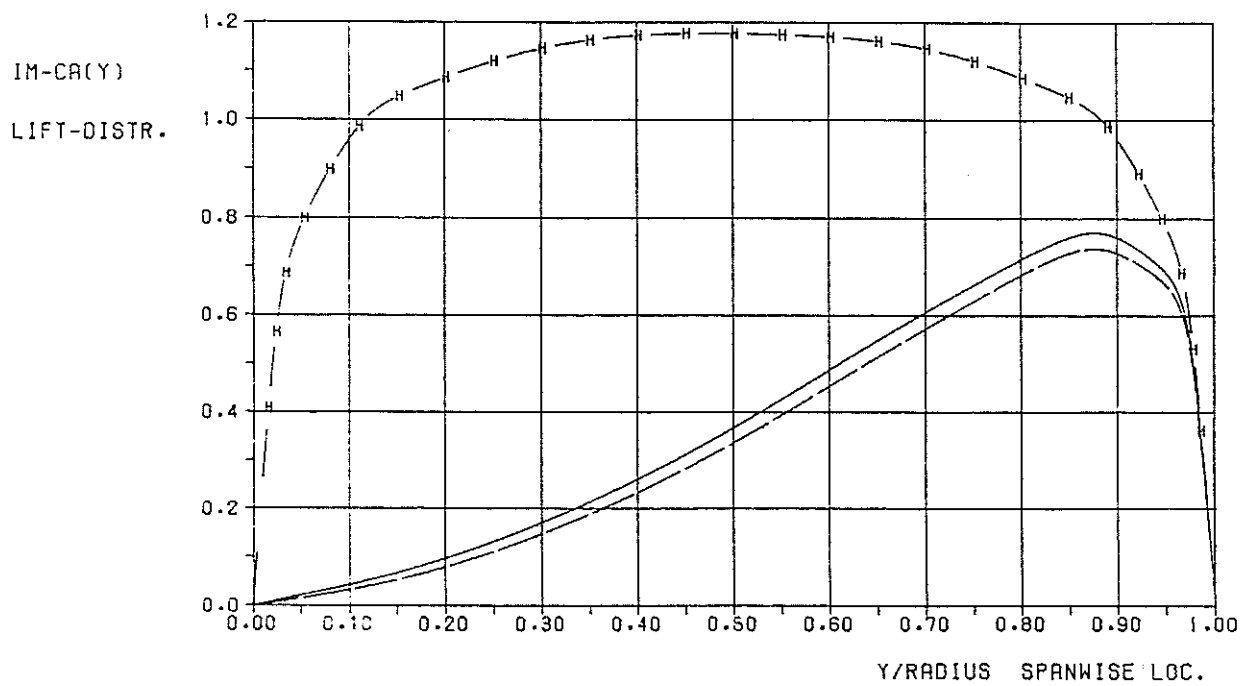
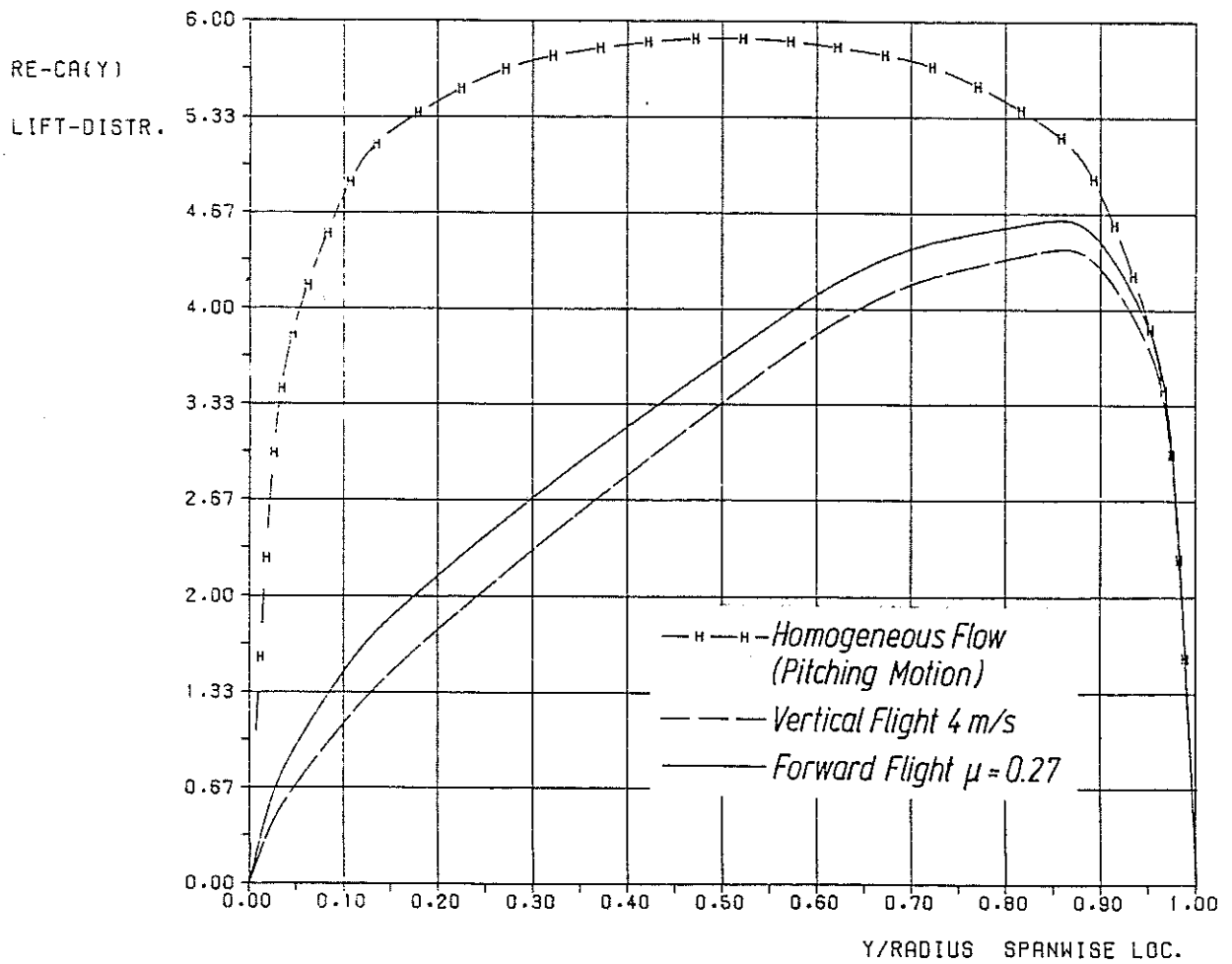


Figure 8: Feathering Motion ($\omega^* = 0.1$)

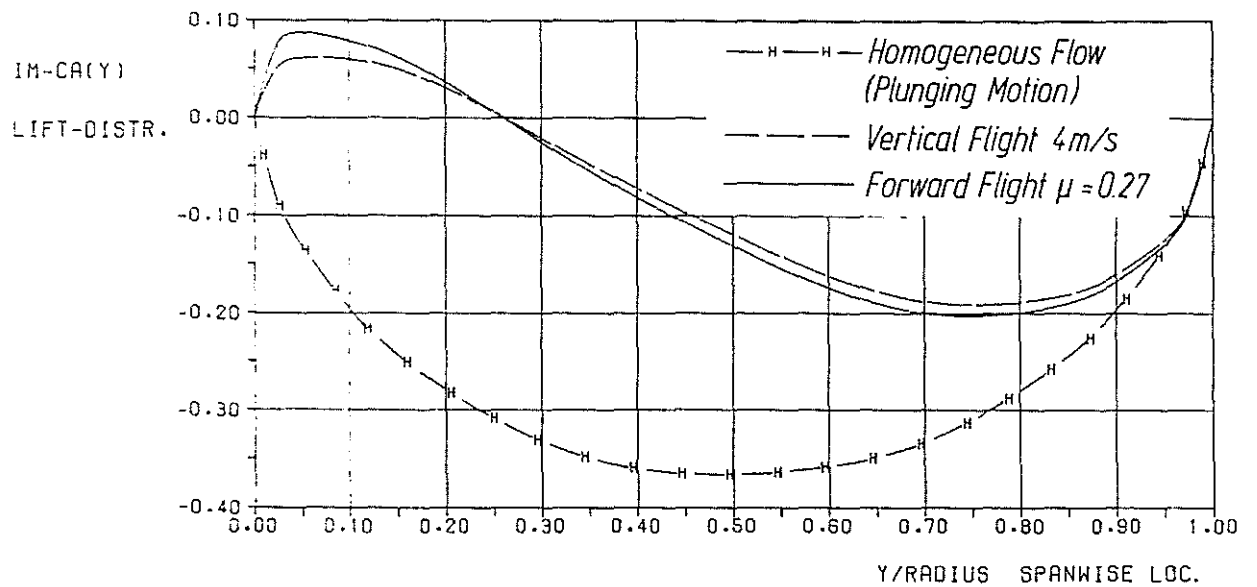
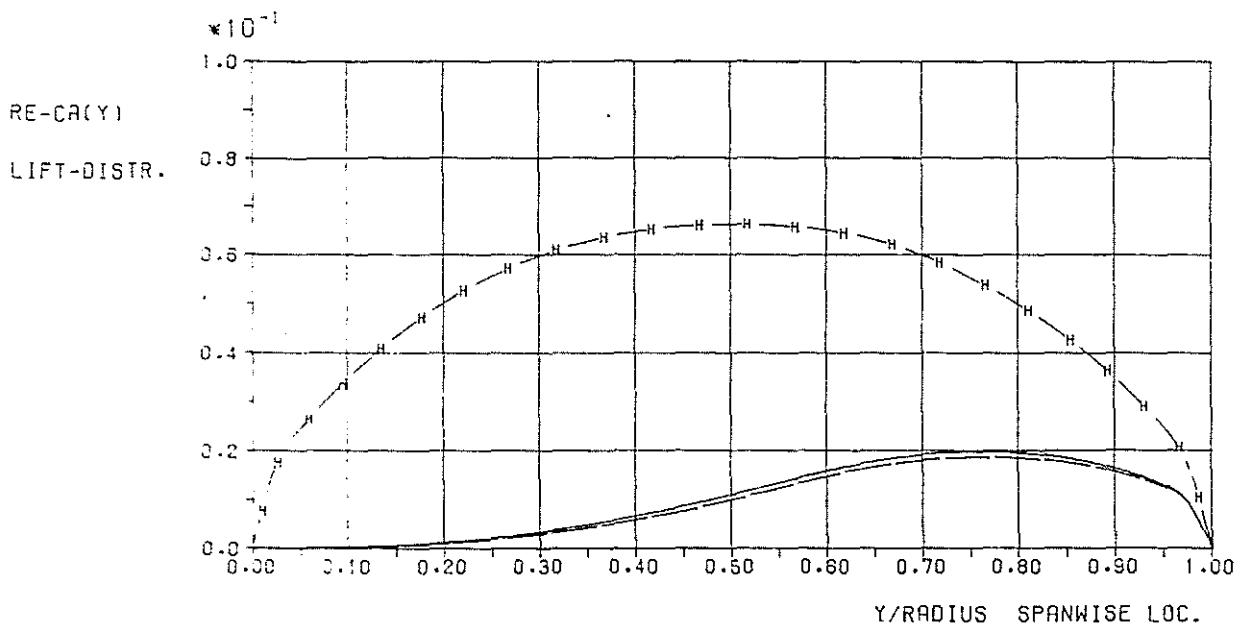


Figure 9: Flapping Motion ($\omega^* = 0.1$)